Electro-Pulse-Enhanced Cancer Therapy

Electro-Pulse-Enhanced Cancer Therapy

By

Bertil R.R. Persson

Cambridge Scholars Publishing

Electro-Pulse-Enhanced Cancer Therapy

By Bertil R.R. Persson

This book first published 2020

Cambridge Scholars Publishing

Lady Stephenson Library, Newcastle upon Tyne, NE6 2PA, UK

British Library Cataloguing in Publication Data
A catalogue record for this book is available from the British Library

ISBN (10): 1-5275-4627-6
ISBN (13): 978-1-5275-4627-1

TABLE OF CONTENTS

ABSTRACT

This book is a summary of my 30 years' experience of electro-pulse-enhanced-therapy in the treatment of malignant tumours.

The first chapter is a short history of the discoveries that led to the clinical use of electro-pulse-enhanced cancer therapy (EpECT). In the late 1960s, Sale found that the action of inducing short electric pulses upon biological cell membranes made them transiently permeable without damaging the membrane structures. In the 1970s, Zimmermann observed that red blood cells began to lose haemoglobin after exposure to a pulsed electric field that exceeded a certain threshold. Exposure to short electrical pulses with amplitudes between 4 and 6 kV/cm resulted in the cells melting together into larger cells containing several nuclei. In the 1980s, Neumann and Wong demonstrated that electrical field-mediated transfer of DNA into cells is a handy technique, simple and easy to apply for DNA transfection. Okino and Mohri reported in 1987 the possibility of using the electroporation effect for enhanced transport of the anticancer drug Bleomycin across the cell membrane. The first clinical trial with EECT was performed on head and neck tumours by L. Mir and colleagues in France, 1991.

The second chapter describes the electrochemical and biophysical principles of the action of high voltage electrical pulses applied to human cells and tissues. The creation of channels in the cell-membrane, usually called electroporation, is the main phenomenon considered in electro-enhanced chemotherapy. However, electrochemical processes may also be involved.

My profession is in medical radiation physics, where radiation dosimetry is the most critical issue in radiation therapy. Thus, I considered it essential to know for certain the amount of energy delivered to the patient in electro-pulse enhanced cancer therapy as well.

The third chapter describes the measurement of the change in the electrical impedance of the tissue as an excellent way to estimate the energy delivered to the tissue through exposure to electrical high voltage pulses.

Another branch of my profession is the use of radio-pharmaceuticals to study the morphology and function of various human organs. As such, the fourth chapter describes the use of radioactive labelled drugs and gamma-camera recording to explore the enhanced uptake of drugs after exposure to electric pulses. Multivariate statistical methods are used to predict the

dependence of drug uptake in the exposed and non-exposed tissue on several variables

The fifth chapter summarizes the results of numerous preclinical studies of electro-pulse enhanced cancer therapy. Bleomycin and Cis-platinum are the drugs mainly used in clinical applications of such therapy. The results of extensive preclinical studies are shown to indicate promising combinations of electro-pulse chemotherapy with established immune therapy and radiation therapy regimes.

As mentioned above, the first clinical trial using Bleomycin and electric pulse treatment (called "electro-chemotherapy" (ECT)) was performed on head and neck tumours by Mir and colleagues in France in 1991. In the following years (up until 2018), clinical trials have treated more than 1500 patients with malignant melanoma, Kaposi´s sarcoma, breast cancer, squamous cell carcinoma, and basal cell carcinoma. The sixth chapter reviews and analyses the clinical results of these trials.

The seventh section discusses the safety concerns that must be taken into account when treating patients with high voltage electrical pulses.

The eighth, and final, part of the book presents a summary of potential new dimensions in electro-pulse enhanced Cancer therapy.

ACKNOWLEDGEMENTS

This book is dedicated to my collaborators in the field of electro-pulse-enhanced cancer therapy (EpECT) over the past 30 years: Leif G. Salford, MD, Professor of Neuro Surgery at Lund University, who opened his laboratory for the first experiments with malignant glioma implanted in rat brains; Louis Mir who supported us with a French electroporation device for animal experiments which led to the publication of "A new brain tumour therapy with EpECT"; Per Henriksson for the "Zero Weed" adventure; Maria Danfelter MSc, for her dedicated pioneering work with cell survival; Per Engström, PhD, for his eminent pre-clinical pioneering work, a strong thesis, and for conducting the first clinical operations with EpECT; Catrin Bauréus-Koch, PhD, for her dedicated work in the extensive rat experiments using radiation and immune therapy combinations, and her exquisite thesis; Gustaf Grafström, PhD, for his skilful operations in the extensive rat experiments; Susanne Strömblad and Catarina Blennow, for their skilful technical assistance in the animal experiments and histology preparations; Bernt Böhmer, engineer and entrepreneur, for his skilful constructions and manufacturing of our various electro-pulse devices; Anders Johnsson, for promoting the gamma camera experiments, and Mohan Frick for bringing electro-pulse-enhanced cancer therapy to the market.

The authors wish to thank the QuickField support team for the temporary license of the program, Version 6.3.2 (Tera Analysis Ltd. http://quickfield.com), without which this work summarized in chapter 3.5 could not have been performed.

CHAPTER I

INTRODUCTION

1.1 ELECTROPORATION OF BIOLOGICAL CELL MEMBRANES

In the late 1960s, Sale found that the action of short electric pulses upon biological cell membranes made them transiently permeable without damaging the membrane structures.[1] When he applied high electric fields up to 25 kV/cm to suspensions of the cells, the potential difference across the membrane of the spherical cell increased. This phenomenon caused conformational changes to occur in the membrane structure, resulting in the loss of its semipermeable properties and lysis of the cells.[2]

Another researcher later found that electric impulses cause transient permeability changes in the membranes of vesicles storing biogenic amines which may lead to stimulated neuro-humoral secretion.[3] Studies of cell membranes in Escherichia coli B163 and B525 demonstrated dielectric breakdown using a Coulter counter, with hydrodynamic jet currents focusing close to the orifice of the counter. By plotting the relative pulse height for compensated amplification of a certain size of the cells against increasing detector current, the transcellular ion flow showed differences for the potassium-deficient mutant B525 in comparison with the wild-type B163, indicating a change in the membrane structure of B525.[4]

Researchers also observed that red blood cells began to lose haemoglobin after exposure to a pulsed electric field when the strength of the field exceeded a certain threshold. The haemoglobin fraction found in the supernatant was designed against the outer electric field strength, and resulted in the classic sigmoid curve characterizing the dielectric decomposition of mammalian cell membranes. They discovered that very short (<1ms), high voltage pulses can dramatically increase the permeability of cell membranes.[5]

Reversible electrical degradation of cell membranes is the fundamental cause of electro-permeabilization (also referred to as electro-injection or electroporation). Local degradation of the cell membrane occurs when the membrane potential exceeds 1V at room temperature and 2V at 4°C. The

breakdown voltage depends on the duration of the pulse. A short pulse (<1 μs) causes transient decomposition at 1V, while a pulse of a longer duration than 10ms causes transient decomposition at 0.5 V. At pulses over 50-100 μs, degradation causes irreversible cellular membrane destruction, leading to cell death.[5,6,7,8,9,10]

1.2 ELECTROFUSION OF BIOLOGICAL CELLS

Exposure of the microorganism *Dictyostelium discoidea* to short (40ps) electrical pulses with amplitudes between 4 and 6 kV/cm resulted in the cells melting together, forming larger cells containing more than 40 nuclei of cells evenly as they lyze.[11]

Red blood cells exposed to an electrically flawed AC with an amplitude of 2.5kV/cm and frequencies between 0.5 and 2 MHz were found to form chains of cells between the electrodes which remain after exposure, and which might lead to a possibility of cell fusion.[12] Zimmerman and colleagues applied this phenomenon to the inclusion of cells of various origins utilizing electrical degradation of cell membranes. This experiment resulted in hybrid cells that joined the properties of two varied cells into a single cell.[13,14,15,16,17,18,19]

The fusion rate of yeast cells treated with polyethylene glycol and Ca^{2+} ions and exposed to a high electric field (2.5 - 5 kV.cm-1) increased by a factor of about 200 for different strains of yeast saccharomyces cerevisiae, as opposed to fusion without electric field exposure. This method enables the production of a large number of cell hybrids for various purposes.[20,21]

1.3 ELECTRO-PULSE ENHANCED DNA TRANSFECTION

Compared to biochemical techniques, electric field mediated transfer of DNA into cells is beneficial, and simple and easy to apply for DNA transfection.[22] When exposing plasmid DNA containing the herpes simplex thymidine kinase (TK) gene and mouse L-cells lacking the TK gene, to electrical fields (8 kV/cm,5μs), a strong expression of TK-DNA was found in the mouse cells.[23] A possible model for the transfer of DNA-plasmids into cells by electroporation is an electro diffusive migration of DNA through the electroporated membrane.[24]

The effects of exposure of biological cells to high-voltage electric pulses have so far been explored in terms of electrofusion used for the production of cell hybrids and monoclonal antibody production, or electroporation induced DNA transport across the cell membrane.[11,25,22,23 5521]

1.4 ELECTRO-PULSE ENHANCED CHEMO-THERAPY *EpEChT*

Okino and Mohri (1987) first reported the possibility of using the electroporation effect for enhanced transport of the anticancer drug across the cell membrane.[26] They treated hepatocellular carcinoma (AH-109A) in rats through an administration of 5 mg of Bleomycin intra-muscularly and exposed the tumours to an electric pulse with an amplitude of 5 kV/cm and a duration of 2 ms. Four days after the treatment, the tumour size had decreased significantly, while tumours treated with electric impulses or Bleomycin alone showed no decrease in growth. Okino and Mohri suggested that electro-enhanced chemotherapy should produce better results than chemotherapy alone.[26,27]

1.5 CLINICAL ELECTRO ENHANCED CHEMO-THERAPY (*EpEChT*)

The first clinical trial with *EpECT* was performed on head and neck tumours by Mir and colleagues in France in 1991.[28] In 1998 the Swedish Radiologist Dr Nordenström at the Karolinska Institute in Stockholm, developed electrochemical therapy (EChT) as a minimally invasive electrotherapeutic technique, using direct current for the treatment of cancer and haemangioma tumours.[29]

Application of electric pulses in vivo used to augment the chemotherapeutic efficiency in cancer treatment has commonly been referred to as electro-chemotherapy and is abbreviated as ECT. However, this abbreviation is also associated with electro-convulsive therapy, as used in psychiatry for the treatment of depression. In this book, *EpECT* is used as an abbreviation for *electro-pulse-enhanced cancer therapy*, while electro-pulse enhanced chemotherapy is abbreviated as *EpEChT*.[30] This latter is a mode of *EpECT* tumour treatment that has been employed mostly for subcutaneous and cutaneous malignancies.[31,32] However, it is also employed to treat soft-tissue sarcomas[33], glioma in the brain[34], liver tumours [35,36,37] and tumours in the pancreas,[38] and has shown auspicious results.

In electro-pulse enhanced chemotherapy treatment, only cells exposed to strong electric fields respond immediately. The permeabilized tumour cells become much more accessible to hydrophilic molecules since the lipophilic membrane barrier generally rejects these. Bleomycin, a very toxic anticancer agent, has proven to be a particularly efficient drug in *EpEChT*, and is by far the most often used, but Cisplatin, another anticancer agent, has also been found to be effective.

Chapter II reviews the electrochemical and biophysical principles of pore formation. In the clinical use of electro-pulse-enhanced chemotherapy, it is important to control the exposure of the patient to an electric field.

Chapter III discusses electro-dosimetry, the measurements of the absorbed energy in a tumour through the electric pulse treatment.

In Chapter IV, radioactive tracers and gamma-camera measurements are employed to explore the effect of the enhanced accumulation of administered drugs in the treatment area.

In Chapter V, various preclinical studies of electro-enhanced cancer therapy are reviewed, as are trials using both Bleomycin, Cis-Platin and other drugs, as well as their combinations.

In chapter VI clinical studies of electro-enhanced cancer therapy using various devices are reviewed, considering both Bleomycin, Cis-Platin, other drugs, and their combinations.

The safety aspects of performing clinical electro-enhanced cancer therapy are discussed in chapter VII. The closing chapters then detail new dimensions of EpECT to summarize the clinical potential in applying electro-pulse treatment to enhance the effect of established cancer therapy regimes.

CHAPTER II

BIOPHYSICAL PRINCIPLES OF *EPECT*

2.1 CELL MEMBRANE

Cell membranes with a thickness of about 7 to 10 nano-m enclose all single cells in the body. The cell membrane is made up of a double layer of phosphorous glycerides, consisting of phosphoric acid and fatty acids (see Figure 2-1a). The end of these molecules with the hydrophilic phosphoric acid (which attracts water) cover each side of the cell membrane, while the other ends of long-chain hydrocarbon chains that are hydrophobic (water repellent) fill the space between the hydrophilic surface layers (see Figure 2-1b).

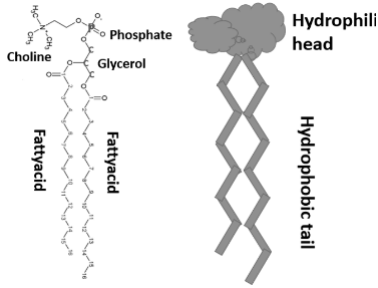

Figure 2-1a
Phosphorous glycerides consisting of phosphoric acid and fatty acids

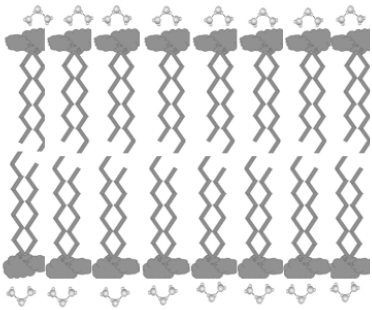

Figure 2-1b
The hydrophilic phosphoric acid (which attracts water) covers each side of the cell membrane, while the other end of long fatty acid hydrocarbon chains that are hydrophobic (water repellent) fills the space between the surface layers.

This structure of the cell membrane creates an electrically insulating double layer of phosphorous glycerides. For the cell to communicate with the environment, there are a large number of various proteins embedded in

the cell membrane. A group of these proteins consists of channel proteins transporting distinct ions through their channels. The difference in concentrations of positive sodium, potassium, calcium ions and negative chloride ions on either side creates a membrane potential that is the basis for the emergence of bioelectric phenomena.

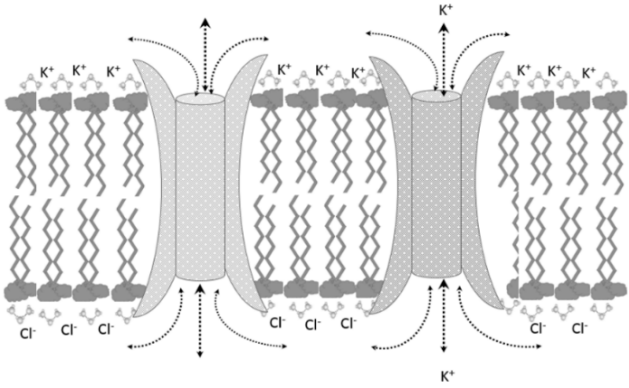

Figure. 2-2
The structure of a cell membrane consists of two lipid layers, with hydrophilic phosphate groups on the surface and hydrophobic fatty acid tails which fill the space inside the membrane. The channel protein embedded in the membrane transports sodium, potassium, calcium and chloride molecules through the membrane. This structure, with differences in ion concentrations on either side of the membrane, generates the membrane potential and the appearance of bioelectric phenomena.

2.2 MEMBRANE POTENTIAL

Differences in the concentrations of ions on opposite sides of a cellular membrane create an electrical potential called the Nernst potential (U_{ion}), determined by the charge on the ion q_{ion} and the ion-concentrations on the inside and outside of the cell.

$$U_{ion} = \frac{R \cdot T}{q_{ion}} \ln \frac{\{ion\ concentration\ outside\ the\ cell\}}{\{ion\ concentration\ inside\ the\ cell\}} \qquad \text{Eq. 2.1}$$

Sodium (Na^+) and chloride (Cl^-) ions appear in high concentrations on the extracellular side of the membrane and in low concentrations on the intracellular side. The concentration of potassium in normal rest conditions is usually about 30-50 times higher inside the cell compared to outside. Potassium ions, therefore, strive to flow out of the cell and accumulate on the outside of the membrane. As the negative charged q^- ions remain in the cell (mainly chloride), accumulating on the inside of the membrane, an electric field directed into the cell develops through the outflow of positively q^+ charged potassium. This condition continues until the force created by the electric field ($\vec{F} = \vec{E} \cdot q^+$), which is directed inwards, inhibits the outbound transport of potassium ions. The electric potential, Φ, is the amount of work needed to move a positive unit charge, $q^+ = 1$, a distance $\Delta\ell$ inside the electric field E without producing any acceleration. The work of moving the K^+ ions a distance $\Delta\ell$ in the E field inside the membrane is thus:

$$\vec{F} \cdot \Delta\ell = \vec{E} \cdot \Delta\ell \cdot q^+ = \Delta\Phi \qquad \text{Eq. 2.2}$$

The potential energy $\Delta\Phi$ is equal to the difference between the membrane potential Φ_M and the Nernst potential for the potassium ion Φ_K , $\Delta\Phi = \Phi_M - \Phi_K$. At equilibrium, the potential energy is zero, $\Delta\Phi = 0$ and $\Phi_M = \Phi_K$.

The general Nernst equation for an arbitrary ion κ is:

$$\Phi_i - \Phi_e = \Phi_\kappa = -\frac{R \cdot T}{q_\kappa \cdot F} \cdot ln \frac{C_I^\kappa}{C_{E,\kappa}}; \ [V] \qquad \text{Eq. 2.3}$$

where

Φi = potential on the inner side of the membrane;
ΦE = potential on the external side of the membrane;
Φ_κ = equilibrium potential for the κ^{th} ion across the membrane $\Phi_i - \Phi_E$ i.e., the Nernst potential U_κ [V];
R = gas constant [8.314 J/(mole·degree Kelvin)];
T = absolute temperature [degree Kelvin];
q_κ = valence of the kth ion;
F = Faraday's constant [$9.649 \cdot 10^4$ As/mole];
C_I^κ = intracellular concentration of the κ^{th} ion;
C_E^κ = extracellular concentration of the κ^{th} ion.

The potential that occurs is called the membrane potential, and is in the order of -40 mV to -70 mV. By introducing a temperature of 37 ° C, which corresponds to T = 273 + 37 °Kelvin, q=+1 for the valence of the potassium ion, and replacing the natural logarithm (ln) with the tenth logarithm ($\log_{10}$), the equation for a monovalent cation (q=+1) can be written as:

$$\Phi = -61 \cdot log_{10} \frac{C_I}{C_E} \ [mV] \qquad \text{Eq. 2.4}$$

- The equilibrium's potential for potassium(q=+1) Φ_K is -88 mV at an intra-cellular potassium concentration of 140mM and an extracellular concentration of 5 mM.
- The equilibrium's potential for sodium(q=+1), Φ_{Na}, is +61 mV at an intra-cellular sodium ion concentration of 14mM and an extracellular concentration of 140 mM.
- The equilibrium's potential for chloride(q=-1), Φ_{Cl}, is -69 mV at an intra-cellular chloride ion concentration of 8mM and an extracellular concentration of 110 mM.
- The equilibrium's potential for calcium(q=+2) Φ_{Ca}, is +140 mV at an intra-cellular calcium ion concentration of 0.1 μM and an extra-cellular concentration of 4mM

The interactions that generate the total rest potential are modelled by the Goldman equation, which is similar to the Nernst equation shown above. The Goldman equation considers the charges of the current ions as well as the difference between their internal and external concentrations. However, it also takes into account every κ^{th} ion's relative permeability $P\kappa$ of the plasma membrane.

$$\Phi_M = \frac{R \cdot T}{F} \cdot ln\left(\frac{P_K \cdot C_E^K + P_{Na} \cdot C_E^{Na} + P_{Cl} \cdot C_I^{Cl}}{P_K \cdot C_I^K + P_{Na} \cdot C_I^{Na} + P_{Cl} \cdot C_E^{Cl}}\right) \qquad \text{Eq. 2.5}$$

In excitatory cells (nerve and muscle cells), the membrane potential is usually around -60 mV.

2.3 MEMBRANE EXPOSED TO ELECTRIC DC FIELD

The electric field E is written as the derivate of the electric potential, Φ,

$E = -\frac{d\Phi}{dr}$ in vector form $\bar{E} = grad\Phi = \nabla\Phi$ Eq. 2.6

Then, by Coulomb's and Gauss's laws, we get Poisson's equation

$E = \frac{1}{4\pi \cdot \varepsilon_o}\frac{q}{r^2} = -\frac{d\Phi}{dr}$; $\frac{dE}{dr} = -\frac{d^2\Phi}{dr^2} \approx \frac{\rho}{\varepsilon_o}$; Eq. 2.7

Alternatively, in vector sign $-\nabla^2\Phi = \frac{\rho}{\varepsilon_o}$; Eq. 2.8

where:

ρ is the charge density (including bound charge)

ε_o is the permittivity = 8.854187817...×10^{-12} F·m^{-1} (farads per metre).

When applying an external electric field, the superposed membrane potential is related to the charge density by Poisson's equation (as in Eq. 2.8). Where no charges are involved, solutions of the Laplace equation (Eq. 2.9) give the electric field in the extracellular and intracellular space.

$$\nabla^2 \Phi = 0 \qquad \text{Eq. 2.9}$$

We assume that the model of a spherical cell according to Figure 2-3 has an inner radius **a** and an outer radius **b** with the membrane thickness **d**. The conductivity of the cell's internal material (cytoplasm) is $\boldsymbol{\sigma_I}$, the cell membrane $\boldsymbol{\sigma_M}$ and the extracellular fluid $\boldsymbol{\sigma_E}$.[5] The electrical potential in the corresponding areas is assumed to be Φ_I, Φ_M, and Φ_E.

Figure 2-3 shows a model of a cell as a layered lossless dielectric sphere subjected to a uniform electric field $\vec{E} = E \cdot \vec{x}$. The concentric outer shell and inner core have conductivities σ_I and σ_M respectively, and the outer radius is b and the inner radius a. The solutions to the Laplace equation (2.9) for the electric potentials in the three regions I, M and E are assumed to be as follows:

$$\Phi_E(\mathrm{r},\theta) = \left(-E \cdot r + \frac{B}{r^2}\right) \cdot \cos\theta \text{; for r > b} \qquad \text{Eq.2.10a}$$

$$\Phi_M(\mathrm{r},\theta) = \left(-B \cdot r + \frac{C}{r^2}\right) \cdot \cos\theta \text{; for b > r > a} \qquad \text{Eq.2.10b}$$

$$\Phi_I(\mathrm{r},\theta) = -D \cdot r \cdot \cos\theta \text{; for r < a} \qquad \text{Eq.2.10c}$$

where

$\Phi_I = 0$, $\Phi_M = A \cdot r \cdot \cos\theta$, and $\Phi_E = \frac{B}{r^2} \cdot \cos\theta$

The border conditions for the two interfaces r =a and r =b are as follows:

$$\Phi_I(a) = \Phi_M(a) \text{ and } \left({}^{\sigma_I}/_{a}\right)\left({}^{d\Phi_I}/_{dr}\right) = \left({}^{\sigma_M}/_{a}\right)\left({}^{d\Phi_M}/_{dr}\right) \qquad \text{Eq. 2.11a}$$

$$\Phi_M(b) = \Phi_E(b) \text{ and } \left({}^{\sigma_M}/_{b}\right)\left({}^{d\Phi_M}/_{dr}\right) = \left({}^{\sigma_E}/_{b}\right)\left({}^{d\Phi_E}/_{dr}\right) \qquad \text{Eq. 2.11b}$$

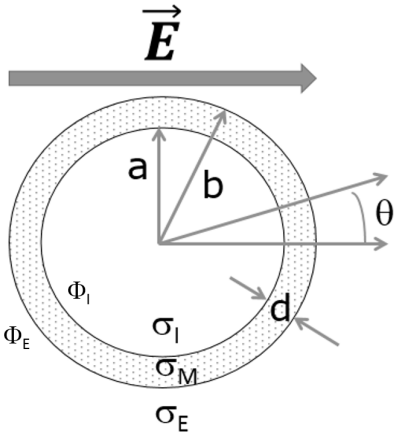

Figure 2-3
An applied external electric field $\vec{E}$ on a spherical cell with the inner radius **a,** and the outer radius **b** with the membrane thickness **d**. The conductivity of the cell's internal material (cytoplasm) is $\boldsymbol{\sigma_I}$, the cell membrane $\boldsymbol{\sigma_M}$ and the extracellular fluid $\boldsymbol{\sigma_E}$.[5]

With these assumptions, the conductivity for the cytoplasm 'σ_I' is about the same as the extracellular space 'i.e.≈ σ_E', and is much larger than the cell membrane 'i.e. >> σ_M'. The Laplace equation gives the following expression for the part of the potential difference $\Delta\Phi_M$ across the membrane depending upon the externally applied electric field E_0 .[5]

$$\Delta\Phi_M = 1.5 \cdot b \cdot E_0 \cdot \cos\theta \qquad \text{Eq.2.12}$$

If, for non-spherical cells, `$1.5 \cdot \cos\theta$´, is replaced by a form factor f, the equation for $\Delta\Phi_M$ becomes:

$$\Delta\Phi_M = f \cdot b \cdot E_0 \qquad \text{Eq.2.13}$$

For a cell with the shape of an ellipsoid of length L and width B, the form factor f becomes f = L / (L - 0.33·B).[5] At an externally applied field strength of 4400 V/cm, which corresponds to a membrane potential of 1.5 V in bovine red blood cells with an average radius of 2.2 μm, a dielectric degradation of the membrane occurred, which caused a 50% leakage of haemoglobin.[5] Cancer cells, which may be 10 times larger in diameter, can achieve the conditions for a dielectric breakdown at a membrane potential of 1.5 V, already around 400 V/cm.[39,40]

2.4 ELECTRIC PULSE PARAMETERS AND FREQUENCY

2.4.1 ELECTROPORATION WITH PULSED AC FIELDS

When an AC-field is applied to cell membranes, the induced trans-membrane potential becomes strongly dependent upon the frequency of the applied field; when the frequency approaches the relaxation time 'τ' of the

membrane. Schwan (1983) derived a relationship from the basic electromagnetic theory for the calculation of the trans-membrane potential '$\Delta\psi_{membrane}$' induced by an oscillating electric field '$E_{applied}$'.[41]

$$\Delta\psi_{membrane} = \frac{1.5 \cdot r \cdot E_{applied} \cdot \cos\theta}{\sqrt{1 + (\omega \cdot \tau)^2}} \quad \text{Eq.2.14}$$

$$\tau = r \cdot C_{membrane} \cdot (\rho_{internal} + \rho_{external}/2) \quad \text{Eq.2.15}$$

where

ω	ω=2πf; Angular frequency (rad.s^{-1})
f	Frequency (Hz)
$C_{membrane}$	Specific capacitance of the membrane (F.m^{-2})
$\rho_{internal}$	Resistivity of the internal medium (Ω.m)
$\rho_{external}$	Resistivity of the external medium (Ω.m)
$E_{applied}$	$=E^0_{applied} \cdot \sin(\omega t)$ Applied field strength V.m^{-1}
t	Time(s)
r	Radius of the cell

The maximum membrane potential induced by an applied AC field is:

$$\Delta\psi^{max}_{membrane} = \frac{1.5 \cdot r \cdot E^0_{applied}}{\sqrt{1 + (\omega \cdot \tau)^2}} \quad \text{Eq. 2.16}$$

$$\Delta\psi^{max}_{membrane} = \frac{1.5 \cdot r \cdot E^0_{applied}}{\sqrt{1 + (2\pi f \cdot \tau)^2}} \quad \text{Eq. 2.17}$$

The concept of electroporation using reactively-coupled AC-fields of kilohertz frequencies is attractive, because it may enable the use of non-invasive electrodes capable of producing electric fields of sufficient strength and depth in tissue to enhance cellular uptake of drugs, thus avoiding the need for invasive needle electrodes, and also reducing the likelihood of painful neural stimulation.

Under physiological conditions, a typical value of the capacitance of the cell membrane is in the order of $C_m = 10^{-2}$ F.m^{-2}. The values of the resistivity values $\rho_{internal}$, $\rho_{external}$ are in the order of 1 Ω.m. The typical radius `r´ of human cells are in the order of r = 10^{-6} -10^{-4} m. Thus, the frequency limits of the low-frequency potential ranges are in the order of 10^2-10^3 kHz.

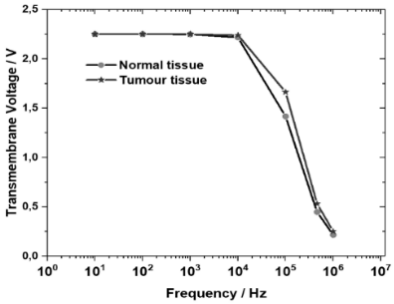

Figure 2-4a
Theoretical calculation of electric-field induced trans-membrane potential, given an applied field strength of 1000 V/cm.

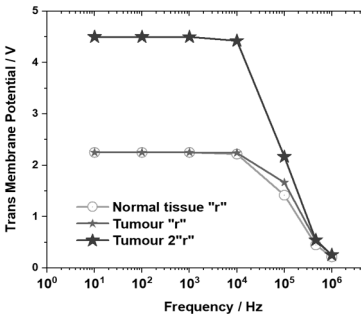

Figure 2-4b
Theoretical calculation of electric-field induced trans-membrane potential, given an applied field strength of 1000 V/cm.

Grosse and Schwan (1992) presented a model for the calculation of cellular trans-membrane potential in the case of very weak electrolytes $\rho >> 1$ Ω.m.[42] This model includes the effect of a variety of factors on transmembrane potential (see Figure 2-3), including medium conductivity and permittivity, cell membrane conductance and permittivity, surface admittance, and space charge effects. Measurements of the *ex vivo* electrical conductivity of a normal human liver and metastatic tumour tissue showed that the conductivity of tumour tissue was significantly higher over the entire frequency range (10 Hz to 1 MHz), with more pronounced differences at lower frequencies.[43]

The Foundation for Research on Information Technologies in Society (ITIS) has an excellent database for the dielectric properties of various human tissues:

https://www.itis.ethz.ch/virtual-population/tissue-properties/database/dielectric-properties/

In Table 2-1, the conductivity (S/m) and resistivity (Ω.m) are given for muscle tissue derived from the ITIS database. According to reported experimental results, the values for tumours are predicted to differ from those for muscles by a factor of about 3 in the frequency range of 10-200 kHz.[44,43] Fitting actual ratios to frequency according to the data of Haemmerich et al. (2009) results in the following Gauss equation:

$$\frac{\sigma_{Tum}}{\sigma_{NT}} = 5.66756 - \frac{10.19901}{2.1077*\sqrt{\pi/2}} * e^{-2*\left[\frac{log_{10}(f) - 5.73715}{2.1077}\right]^2} \quad \text{Eq. 2.18}$$

where:

σ_{Tum}	= Conductivity of tumour tissue;	S/m
σ_{NT}	= Conductivity of normal muscle tissue;	S/m
f	= Frequency;	Hz

In Table 2-1, the conductivity values for muscle tissue are derived from the ITIS database, and estimated values for tumour tissue are provided by applying the equation Eq. 2.18 to the muscle tissue data.

Table 2-1
The conductivity (S/m) and resistivity (Ω.m) for muscle and tumour tissue.

Frequency kHz	Muscle S/m	Tumour S/m	Muscle Ω.m	Tumour Ω.m
10	0.341	1.594	2.933	0.627
20	0.345	1.429	2.899	0.700
40	0.350	1.227	2.857	0.815
80	0.358	1.018	2.793	0.982
100	0.362	0.957	2.762	1.045
110	0.364	0.933	2.747	1.072
120	0.366	0.911	2.732	1.097
140	0.370	0.876	2.703	1.141
180	0.379	0.830	2.639	1.205
200	0.384	0.815	2.604	1.226

The equations for normal muscle tissue conductivity variation with frequency fitted to the data of the ITIS database in the frequency f interval 1 - 4000 Hz are as follows:

$$\sigma_m = 0.2 + 0.00003 \cdot f \text{ S/m} \quad \text{Eq.2.19}$$

In the frequency f interval 4000 – 200 000 Hz:

$$\sigma_m = 0.337 + 3.49 \cdot 10^{-7} \cdot f - 1.45 \cdot 10^{-12} \cdot f^2 + 4.49 \cdot 10^{-18} \cdot f^3 \text{ S/m} \quad \text{Eq.2.20}$$

In Figure 2-4a, calculations are based on Eq. 2.17 with data for normal tissue cellular radius r = 15 μm, and $C_m = 0.001$ F.m^{-2}; $\rho_{in} = 10$ Ω.m; $\rho_{ex} = 15$ Ω.m. For tumour cellular radius r = 15 μm, and $C_m = 0.001$ F.m^{-2}; $\rho_{in} = 3.3$ Ω.m; $\rho_{ex} = 15$ Ω.m.[43]

In Figure 2-4b, calculations are based on Eq. 2.17 with normal tissue data for cellular radius r = 15 μm.
Cm = 0.001 F.m^{-2}, ρ_{in} = 3.5-13 Ω.m, ρ_{ex} =15 Ω.m, and with tumour tissue data for cellular radius r = 15 μm or 30 μm, C_m = 0.001 F.m^{-2}, ρ_{in} = 1.9-2.4 Ω.m, and ρ_{ex} =15 Ω.m. [43]

In agreement with experimental findings, the theoretical model also predicts that a trans-membrane voltage of sufficient magnitude to cause electroporation appears at an applied field strength of 1200 V/cm at 20 kHz.[45]

A study by Chen et al. (2008) showed that 20–160 kHz in electric fields of peak amplitude 700–2000 V/cm, when applied as a series of short pulses, induce electroporation in cell membrane.[46] Increasing the field strength above 1100 V/cm results in higher cell electroporation efficiency, but increases cell death. In the study, total electroporation yield is only weakly dependent on the frequencies in the frequency range used, although the results suggest a peak of Calcein uptake at 60 kHz. For the parameter values chosen, AC and DC electroporation produced similar yields. Marszalek et al. (1990) studied electroporation in a murine myeloma cell line using AC fields, in the frequency range 100–300 kHz and with field strengths between 500 V/cm and 1500 V/cm.[45]

The study identified a threshold electric field around 600 V/cm using a single pulse of 200ms. However, the article gives no quantitative information about electroporation efficiency and cell viability. The threshold field strength for electroporation in the study of Marszalek et al. (1990) was approximately half of that found through the study by Chen et al. (2008).[45,46]

This result may be due to several factors, including differences in the conductivity of the extracellular medium, pulsing regime, the geometry of the electrodes, the chemistry used to detect electroporation, and cell lines.

The results of Chen et al. (2008) offer conclusive evidence of electroporation using pulsed with AC fields beyond the kilohertz range. The results also suggest an optimal frequency range of 40–120 kHz at a field strength of 1700 V/cm and total exposure time 40ms.[46]

Influenced by these findings of an optimal frequency window for electroporation achievements, the author analysed the frequency content of the various pulse sequences usually used in the protocols for electro-enhanced chemotherapy.

A recent investigation of electroporation with 5 ms bursts of sinusoidal signals in the frequency range of 8 -130 kHz showed that permeabilization appeared at about 100% up to 50 kHz, and then drastically decreased to

about zero above 130 kHz.[47] This result is in solid agreement with the results of the theoretical calculations displayed in Figure 2-4.

2.4.2 FOURIER ANALYSIS OF *EpECT* PULSES

The **Fourier analysis** decomposes a pulse V(t) in the time domain, into the frequencies f that make up a frequency distribution G(f).

A. A SINGLE RECTANGULAR PULSE

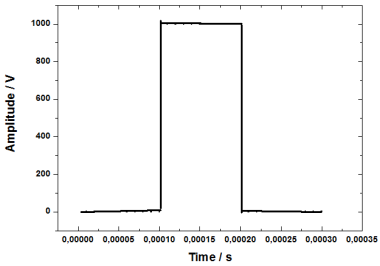

Figure 2-5a
Single rectangular pulse of 1000 V amplitude, and 100µs pulse-length

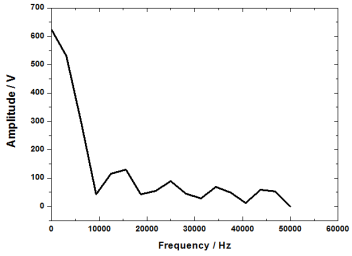

Figure 2-5b
The positive frequency content of the single rectangular pulse in Figure 2-5a

The result of the Fourier analysis of a single rectangular pulse according to the ESOPE protocol displayed in Figure 2-5b shows that the main content of frequencies is in the low energy range < 1 kHz. In the region of optimal electroporation (30- 120 kHz), there is only a minor content of frequencies.

B. A PULSE-TRAIN OF RECTANGULAR PULSES

The result of the Fourier analysis of a pulse train of a rectangular pulse according to the ESOPE protocol displayed in Figure 2-6b shows that there is a peak at 5 kHz corresponding to the 200µs wavelength. There is, however, still a large amplitude at low frequencies, which causes nerve excitation and pain, which this study attempted to avoid by using a 5 kHz pulse-train. In the region of optimal electroporation 30 - 120 kHz, there is still only a minor content of frequencies.

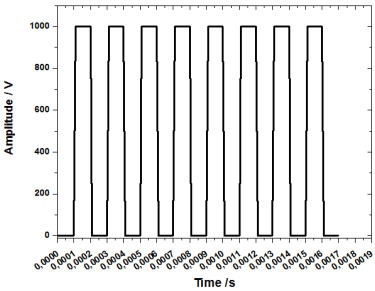

Figure 2-6a
Pulse-train of 8 rectangular pulses of 1000 V amplitude. 100μs pulse-length and 200 μs wave-length (5 kHz).

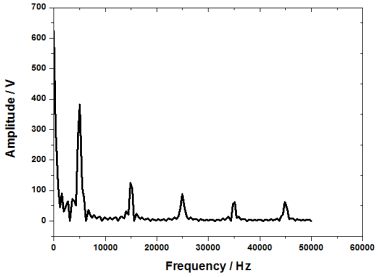

Figure 2-6b
The positive frequency content of the pulse-train of 8 rectangular pulses in Figure 2-6a

The conductivity for healthy muscle tissue averaged over the positive frequency spectrum of Figure 2-6b for each pulse of the pulse train becomes 0.30 S/m. The specific energy thus delivered to a pulse train of 8 rectangular pulses of 1000 V amplitude and 100μs pulse-length is 2208 J/kg. By applying Eq.2.17, the conductivity of tumour tissue conductivity was estimated to be 1.68 S/m, and the specific energy delivered to a pulse train was put at 12514 J/kg.

C. A SINGLE EXPONENTIALLY DECREASING PULSE

Figure 2-7b displays an exponentially decreasing pulse of 139 μs half-time, 1000 V maximum amplitude, and 100μs pulse-length. The result of the Fourier analysis in Figure 2-7b shows that the main content of frequencies is in a broad peak around 7 kHz, with a substantial contribution in the region of optimal electroporation 30 - 120 kHz.

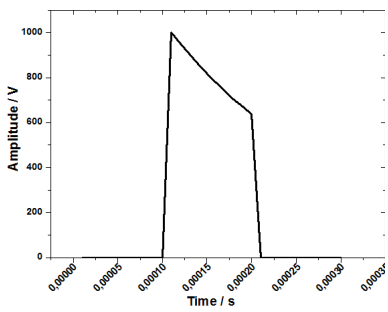

Figure 2-7a
An exponentially decreasing pulse of 139 μs half-time, 1000 V maximum amplitude, and 100μs pulse-length.

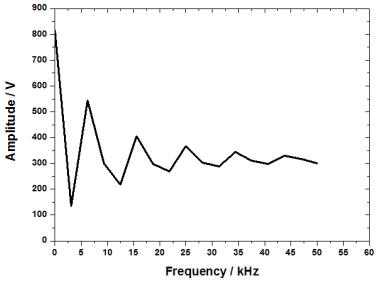

Figure 2-7b
The positive frequency content of the single exponentially decreasing pulse in Figure 2-7a.

D. A PULSE TRAIN OF EXPONENTIALLY DECREASING PULSE

Figure 2-8a displays a pulse-train of 8 exponentially decreasing pulses of 139 μs half-time, 1000 V maximum amplitude, and 100 μs pulse-length. The result of the Fourier analysis displayed in Figure 2-8b shows that the main content of frequencies is in a peak around 5 kHz corresponding to the pulse repetition frequency, and that there are several peaks with a minor contribution in the region of optimal electroporation 30- 120 kHz.

The conductivity for healthy muscle tissue averaged over the positive frequency spectrum of Figure 2-8b for each pulse of the pulse train becomes 0.34 S/m. The energy thus delivered to a pulse train of 8 exponentially decreasing pulses of 139 μs half-time, 1000 V maximum amplitude, and 100 μs pulse-length is 2030 J/kg. By applying Eq.2.17, the conductivity of tumour tissue conductivity was estimated at 1.94 S/m and the specific energy delivered to a pulse train was put at 11 500 J/kg.

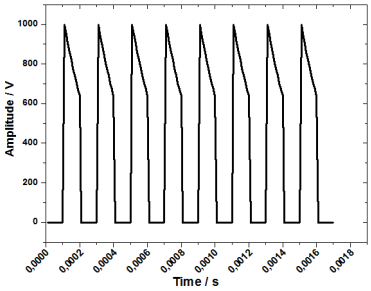

Figure 2-8a
Pulse train of 8 exponentially decreasing pulses of 139 μs half-time, 1000 V maximum amplitude and 100μs pulse-length.

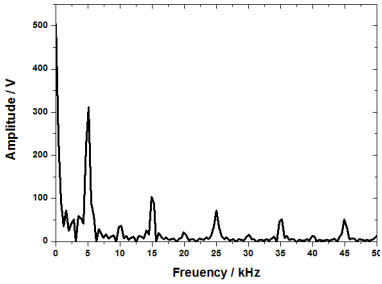

Figure 2-8b
The positive frequency content of the exponentially decreasing pulse in Figure 2-8a.

E. SINGLE SINUSOIDAL PULSE AT 10 kHz

Figure 2-9a displays a single sinusoidal pulse of ±1000 V max amplitude and 9677.5 Hz frequency corresponding to 103 μs pulse-length. The result of the Fourier analysis displayed in Figure 2-9b shows that the main content of frequencies is in a peak around 10 kHz, with a minor contribution of overtones at a higher frequency.

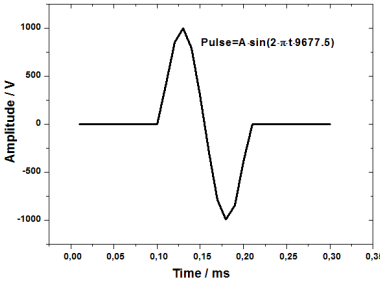

Figure 2-9a
A sinusoidal pulse of ±1000 V max amplitude and 9677.5 Hz frequency corresponding to 103 μs pulse-length.

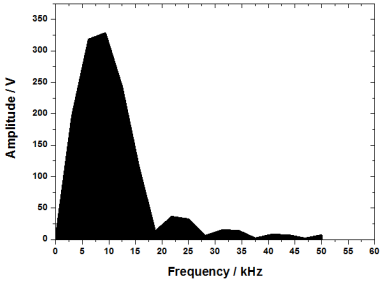

Figure 2-9b
The positive frequency content of the sinusoidal pulse in Figure 2-9a.

F. PULSE TRAIN OF 10 KHZ SINUSOIDAL PULSES

Figure 2-10a displays a pulse train of 8 sinusoidal pulses of ±1000 V max amplitude and 9677.5 Hz frequency corresponding to 103 μs pulse-length. The result of the Fourier analysis displayed in Figure 2-10b shows that the main content of frequencies is in one peak around 5 kHz corresponding to the pulse train frequency and another peak at 10 kHz corresponding to the frequency content of the single pulses. There is also a third peak corresponding to the overtone of the sinusoidal pulse. There are minor contributions in the regions of low frequencies <1 kHz and of optimal electroporation 30 - 120 kHz.

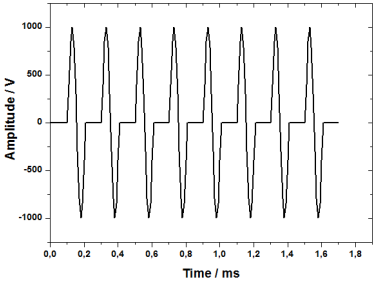

Figure 2-10a
Pulse-train of 8 sinusoidal pulses of ±1000 V max amplitude and 9677.5 Hz frequency corresponding to 100 μs pulse-length.

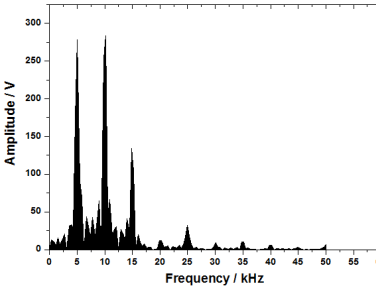

Figure 2-10b
The positive frequency content of the pulse-train of 8 sinusoidal pulses in Figure 2-10a.

The conductivity for healthy muscle tissue averaged over the positive frequency spectrum of Figure 2-10b for each pulse of the pulse train becomes 0.34 S/m. The energy thus delivered to a pulse train of 8 sinusoidal pulses of ±1000 V max amplitude and 9677.5 Hz frequency corresponding to 100 μs pulse-length is 1409 J/kg. Thus, this pulse train must have 14 pulses to deliver the same energy as the ESOP protocol of 8 rectangular pulses of 100 μs at 5 kHz.

2.5 ELECTRO-PORES CREATION AND EVOLUTION FOR DRUG DELIVERY

The application of external electrical fields to biological cells creates initially hydrophobic pores at a rate depending on the absorbed energy.[48,49,50] Smaller pores of radius r < 0.5 nm are rapidly sealed, while

larger ones are stable hydrophilic pores with a radius > 0.8 nm.[51] The rate of formation of such stable pores is modelled by the following equation.[51, 52]

$$\frac{dN}{dt} = \alpha \cdot e^{(\Phi_M/\Phi_{Ep})^2} \cdot \left(1 - \frac{N}{N_{eq}(\Phi_M)}\right) \qquad \text{Eq. 2.21}$$

where

N = Pore density (m^{-2})

α = Creation rate coefficient ($1 \cdot 10^9$ $m^{-2}.s^{-1}$)

ϕ_M = Membrane potential

ϕ_{Ep} = Threshold potential for electroporation ≈258 mV

$N_{eq}(\phi_M)$ = Pore density at membrane potential ϕ_M given by Eq. 2.22

N_0 = $1.5 \cdot 10^9$ (m^{-2}).[51]

$$N_{eq}(\Phi_M) = N_o \cdot e^{2.46 \cdot (\Phi_M/\Phi_{Ep})^2} \qquad \text{Eq. 2.22}$$

The bilayer energy W_M of a membrane with K electro-pores of an initial radius r_j depends on the following parameters: [53]

1. Steric repulsion of lipid heads $\sum_{j=1}^{K} \beta \cdot \left(\frac{r_s}{r_j}\right)^4$;
2. Edge energy of the pore perimeter $\sum_{j=1}^{K} 2\pi\gamma r_j$;
3. The effect of the pores on the membrane tension ; where $\sum_{j=1}^{K} -\pi \cdot \sigma_{eff}(A_p) \cdot r_j^2$; $\sigma_{eff}(A_p)$ is a function of the combined area of pores $A_p = \sum_{j=1}^{K} \pi r_j^2$;
4. Contribution to the membrane potential $\sum_{j=1}^{K} \int_0^{r_i} F(r_j \Phi_M) \cdot dr$.

As the electro-pores expand their total area and ($A_p = \sum_{j=1}^{K} \pi r_j^2$) increases, the effective membrane tension σ_{eff} felt by each pore decreases according to the equation:[54]

$$\sigma_{eff} = 2 \cdot \sigma' - \frac{2 \cdot \sigma' - \sigma_o}{(1 - A_p/A_M)^2} \qquad \text{Eq. 2.23}$$

where

σ' is the specific tension energy (0.02 $J.m^{-2}$) of the hydrocarbon-water;

σ_o is the specific tension energy without pores (0.01$J.m^{-2}$);

A_M is the total area of the cell membrane ($1.26 \cdot 10^{-9}$ m^2 of a cell with a 10 μm radius).

The electric force $F(r.\Phi_M)$ acting on a pore of a toroidal inner surface according to Fig 2-11 is given by Eq. 2.24.[54]

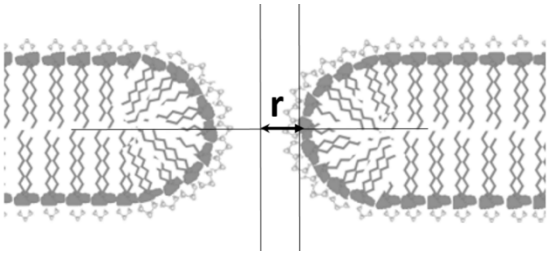

Figure 2-11
Schematic illustration of an electro-pore of radius **r** in the cell membrane

$$F(r.\Phi_M) = \frac{F_{max}}{1 + \frac{0.97 \cdot 10^{-9}}{r + 0.31 \cdot 10^{-9}}} \cdot \Phi_M^2 \qquad \text{Eq. 2.24}$$

where

F_{max} is the maximum of electric force ($0.7 \cdot 10^{-9}$ N.V^{-2} at Φ_M= 1 V).

Thus the energy W of the entire membrane lipid bilayer is:[54]

$$W=\sum_{j=1}^{K}\left\{\beta \cdot \left(\frac{r_s}{r_j}\right)^4 + 2\pi\gamma r_j - \pi \cdot \sigma_{eff}(A_p) \cdot r_j^2 + \int_0^{r_i} F(r_j\Phi_M)\, dr\right\} \qquad \text{Eq. 2.25}$$

The radius of a pore with an initial radius r_j increases in size while the membrane energy is degrading according the following equation:

$$\frac{dr_j}{dt} = -\frac{D}{kT} \cdot \frac{dW_M}{dr_j} \cdot \text{j} = 1,2,,,,,\text{K} \qquad \text{Eq. 2.26}$$

where $\frac{dW_M}{dr_j}$ is the rate of degrading the bilayer energy W_M of a membrane with K expanding electro-pores of an initial radius r_j.

2.6 DRUG DELIVERY THROUGH THE ELECTRO-PORES

The number of pores at the end of the electroporation pulse N_p is estimated by integrating the electro-pore density over the entire cell surface. Data on the effect of field strength from 130 V/cm to 1000 V/cm on a total number of pores distributed over the cell surface have been extracted from the diagrams in *Figure 8* of the work of Krassowska and Filev (2007).[55]

The average pore radius at the end of electroporation is assumed to be r_p, and thus the total cross-section area of electro-pores is $A_p = K \cdot \pi \cdot r_p^2$. As soon as the applied electroporation pulse ends, the created pores start to reseal at a first-order rate with mean decay time τ_p in the order of seconds (Figure 2-12).

$$A_p = K \cdot \pi \cdot r_p^2 \cdot e^{-t/\tau_p} \qquad \text{Eq. 2.27}$$

In an exploration of the enhanced uptake of the radioactive tracer in rats after applied electric pulses of 1000 V/cm field-strength and 100μs pulse-length, the relaxation time τ of the bio-impedance was examined as well.[56] The radioactive tracer ^{99m}Tc-DTPA was administered as a depot intramuscularly (i.m.) in the shoulder of Fischer-344 rats in several fractions of 50 μl each, in 1-minute intervals. Treatment with electric pulses was performed with 2 needle electrodes separated by 8 mm and inserted in the right posterior thigh muscle, through which pulses of 600; 800; 1000;1 200 V/cm field-strength (of 100, 250, and 500 μs pulse-length) were applied. At 6 and 24 hours after electro pulse treatment, a gamma-camera recorded the distribution of ^{99m}Tc-DTPA in the rats.

Before applying the pulse treatment, two measurements of the conductance performed at 2 and 20 kHz through the needle electrodes in the right posterior thigh muscle established the reference level G_{before}. Then, during the treatment, measurements of the conductance took place between each consecutive pulse (Np = 2,4,6,10,12) applied at 1s intervals.

After the last applied pulse, the final conductance G_{after} started to decrease and approach a plateau value. To study the relaxation of the created pores, the conductance measurements were continued 15 seconds after the last pulse at 1s intervals.

The plateau value relative to the conductivity G_{after} that was reached after 15s is a measure of the fraction of reversible electro-permeabilized cells. This value is of importance for the long-term transfer of exogenous substances to the cell and the outflow of immunogenic substances from the cell. Figure 2-12 displays the relaxation curve fitted to the following equation of single exponential decay:

$$G(t) = G_{end}\cdot(f_{irr} + f_{rev}\cdot exp(-t/\tau_p) \qquad \text{Eq.2.28}$$

where

f_{rev} is the fraction of reversible electroporation;
f_{irr} is the fraction of irreversible electroporation;
τ_p is the mean relaxation time.